PAPER

Check for updates

Rapid capture of trace precious metals by amyloid-like protein membrane with high adsorption capacity and selectivity†

Facui Yang,‡[a] Zhigang Yan,‡[b] Jian Zhao,[a] Shuting Miao,[a] Dong Wang[c] and Peng Yang [ID] *[a]

Current technologies for recovering precious metals suffer from high energy consumption, poor adsorption selectivity, slow adsorption kinetics, poor recyclability and expensively complex recovery processes. Thus, there is an urgent need to develop an ecofriendly system to recover precious metals from resources (*e.g.*, ores, waste electrical components or wastewater) with high capacity and low cost. Here, we report a protein-based bilayer membrane made from the one-step aqueous self-assembly of phase-transitioned lysozyme that can efficiently sequester gold ions from dilute aqueous solutions (0.1 to 400 ppm). Notably, this membrane, with a special design of top microparticles and bottom nanomembrane layers, has a cost comparable to that of activated carbon, and exhibits an adsorption capacity for gold of 1034.4 mg g^{-1}, which is 3–15 times higher than those of the most-utilized industrial adsorbents, such as activated carbon and ion exchange resins. The high adsorption capacity for gold could be further extended to other primary precious metals, and high selectivity towards precious metals was simultaneously maintained when extracting precious metals at <1 ppm from ores or waste electrical leachate solutions containing a large amount of competing metal ions. Without the extra addition of any reductants, the membrane could be further directly used to reduce the adsorbed gold ions, affording gold with a final purity of 23 K (95.8 wt%) after pyrolysis.

Introduction

Steadily increasing demand for precious metals, especially Au, Ag and platinum group metals (Pd, Pt, Rh, Ir, Ru and Os), has resulted in the scale-up of metal extraction and refining operations worldwide.[1–3] With the decrease in or exhaustion of rich mineral resources, how to collect precious metals from low-grade mineral resources, municipal solid waste (MSW), waste electrical and electronic equipment (WEEE) or industrial wastewater has become a cutting-edge research topic.[4–6] Adsorption has been considered a promising technology to recover trace precious metals from wastewater due to its low cost and easy operation.[7,8] The most widely used adsorbent for precious metals is activated carbon.[9] Although activated carbon prepared from coal or biomass has good adsorption performance, the production of activated carbon requires high-temperature activation (>500 °C) and acidification, which results in high energy demand (97 MJ kg^{-1}) and the generation of the greenhouse gas carbon dioxide (6.6 kg CO$_2$ eq. per kg).[10] In addition, the regeneration process of activated carbon is reported to further require approximately 50% of the energy demand of activated carbon during its production.[11] Alternative environmentally friendly adsorbents have been developed, such as microorganisms and biomass materials.[12–16] Both of these recovered materials also suffer from main problems: they have a low adsorption capacity, require an extensive adsorption time, have a high cost and cannot be applied on a large scale. For example, although studies have demonstrated the selective adsorption of Au^{3+} and Pd^{2+} from industrial wastewater by using native proteins such as lysozyme, bovine serum albumin (BSA) and ovalbumin,[17] these native proteins with a high denaturation probability, are not easy to collect after adsorption and have low adsorption capacity. Recent work has shown that amyloid fibrils play a potential role in the removal of metal ions. For example, amyloid fibril-activated carbon hybrid membranes can be used for the removal of metal ion pollutants from water by filtration.[18] Nevertheless, the extraction was only demonstrated in single metal ion solution, and preparation of amyloid fibrils requires high temperature, strong acid and a reaction time of tens of hours with a dependence on organic/inorganic additives.

[a]Key Laboratory of Applied Surface and Colloid Chemistry, Ministry of Education, School of Chemistry and Chemical Engineering, Shaanxi Normal University, Xi'an 710119, China. E-mail: yangpeng@snnu.edu.cn

[b]Department of Orthopaedics, Beijing Longfu Hospital, Beijing 100010, China

[c]School of Mechanical and Precision Instrument Engineering, Xi'an University of Technology, Xi'an 710048, China

† Electronic supplementary information (ESI) available: Experimental section; supporting figures and tables. See DOI: 10.1039/c9ta12124b

‡ Facui Yang and Zhigang Yan contributed equally to this work.

3438 | *J. Mater. Chem. A*, 2020, **8**, 3438–3449

This journal is © The Royal Society of Chemistry 2020

Here, we report a fundamental breakthrough in demonstrating a pure protein-based bilayer membrane prepared by lysozyme self-assembly that can be used as an efficient adsorbent for the extraction and recovery of precious metals following chemisorption-based pseudo-second-order kinetics and the Freundlich model. The protein-based bilayer membrane, with a special design of top microparticle and bottom nanomembrane layers, has a cost comparable to that of activated carbon and mild aqueous fabrication/regeneration conditions, and exhibits an adsorption capacity for gold of 1034.4 mg g^{-1}, which is significantly higher than those for activated carbon, ion exchange resins, metal–organic frameworks (MOFs) and other existing adsorbents (*e.g.*, bacteria, fungi, algae and other biomass materials). We further demonstrate the selective adsorption of primary precious metals from aqueous leaching solutions of ore and WEEE at low concentrations (<1 ppm) using the protein bilayer membrane, and 90% of precious metals (Au, Pd, Pt, Ir, Ru and Os) could be selectively extracted from the mixed system under 30 min in the presence of large amounts of competing common metal ions and anions. In contrast to existing systems requiring the exogenous addition of reducing agents (*e.g.*, sodium borohydride or sodium citrate), a high pH (pH > 10) and slow reduction rate (over ten hours),[19,20] the adsorbed gold ions on the membrane surface could be spontaneously reduced at room temperature in the absence of any other reductants, showing a rapid reduction ratio of 90% from Au^{3+} to Au^{+} in 10 min and a gold purity of 23 K (95.8 wt%) after pyrolysis. The high adsorption capacity (3–15 times higher than that of activated carbon and ion exchange resins), selectivity and rapid reduction capability come from the multilevel cooperation between amino acid residues exposed on the membrane surface and precious metal–chloro complex anions in acidic solution, typically including adsorption by electrostatic interaction, reduction by tryptophan and stabilization by cysteine.

Results and discussion

Preparation of the protein-based adsorbent

The fabrication process of the bilayer membrane is shown in Fig. 1a. When lysozyme was dissolved in HEPES buffer (pH 7.0) with the addition of tris(2-carboxyethyl)phosphine (TCEP), a rapid lysozyme conformation change occurred after its disulfide bonds were broken down by TCEP, inducing the heterogeneous nucleation and assembly of lysozyme.[21,22] In this protein phase-transition process, an abundance of unfolded protein monomers (phase-transitioned lysozyme, PTL) were formed in a few minutes, which subsequently facilitated assembly into substantial oligomers and protofibrils. The superfast aggregation of oligomers driven by β-sheet stacking resulted in the formation of a nanomembrane at the solid/water interface. Meanwhile, the oligomers in bulk solution further propagated very quickly to protofibrils, which subsequently aggregated and fused into microparticles deposited on the nanomembrane surface.[23] This process led to a bilayer membrane at the solid/water interface. The membrane was cross-linked with glutaraldehyde (1 wt%) for 30 min at room temperature so that the microparticles could be stably tethered on the nanomembrane by this cross-linking agent. Then, the membrane was detached from the glass after soaking in 1 M NaOH solution for 1 h due to the corrosion of the glass by sodium hydroxide.[24] Fig. 1b shows the structure of the bilayer membrane: the bottom was the nanomembrane (thickness: ~260 nm), and the top was closely packed microparticles (size: 500 nm to 1 μm). Hence, the nanomembrane provided structural support for the microparticles that were stably fixed on the nanomembrane.

Since the adsorption capacity of an adsorbent is typically evaluated as the adsorption per unit mass, the protein concentration that would significantly affect the mass of the PTL membrane was determined to be 30 mg mL^{-1}, and this value was not changed unless specifically noted. Instead, the pH and concentration of TCEP buffer were adjusted, which did not noticeably change the resultant membrane mass but effectively modulated the membrane thickness and Brunauer–Emmett–Teller (BET) specific surface area. For instance, the membrane thickness and corresponding BET surface area could be regulated from 5 to 24 μm and 3.6 to 10.5 m^2 g^{-1}, respectively, by simply increasing the TCEP concentration from 15 to 50 mM (Fig. 1c, d, S1 and S2, ESI†). While a high concentration of TCEP solution intensified the reaction extent to afford a thick membrane with a large BET surface area, a TCEP solution pH above 6 also showed a positive effect on the membrane thickness and BET surface area (Fig. 1c and d). Amyloid aggregation was enhanced by increasing the pH to approach the pI of the protein (11 for lysozyme) due to the attenuation of electrostatic repulsion among the colloids.[23] As a result, the membrane thickness and BET surface area decreased to 10 μm and 7.4 m^2 g^{-1}, respectively, at a low pH of 6, and then increased to approximately 24 μm and 10.6 m^2 g^{-1} from pH 6 to 11 (Fig. 1c, d, S3 and S4, ESI†).

The functional groups on the membrane surface mainly included aliphatic carbon (C–H/C–C), amines (C–N), hydroxyls (C–O), thiols (C–S), amides (O=C–N) and carboxyl groups (O=C–O), as reflected by X-ray photoelectron spectroscopy (XPS) of the membrane surface (Fig. S5, ESI†).[25] These multiple functional groups on the membrane provided binding sites for metal ions.[26,27] We then expected that the PTL bilayer membrane could be used for the adsorption and rapid reduction of gold ions. For the initial evaluation, chloroauric acid (HAuCl$_4$) was chosen as the ionic Au source due to the expected attraction of the [AuCl$_4$]$^{-}$ ion to the positively charged lysozyme with an isoelectric point (pI) of 11. To some extent, the effect of the pH and concentration of the TCEP buffer on the membrane thickness and BET surface area could also result in modification of the adsorption ratio (R_A, see ESI† for details) for gold ions (Fig. 1e). For instance, the low thickness and BET surface area at 15 mM TCEP and pH 6 resulted in a relatively low R_A at 40–75%, while the increased thickness and BET surface area at TCEP > 15 mM and pH 7–9 led to a high R_A above 95%. A sudden drop in R_A from 85% to 40% was observed at TCEP pH > 10, which might be due to the attenuation of electrostatic interactions between gold ions and the weakly charged membrane surface, which was prepared at a pH (>10) close to the pI.
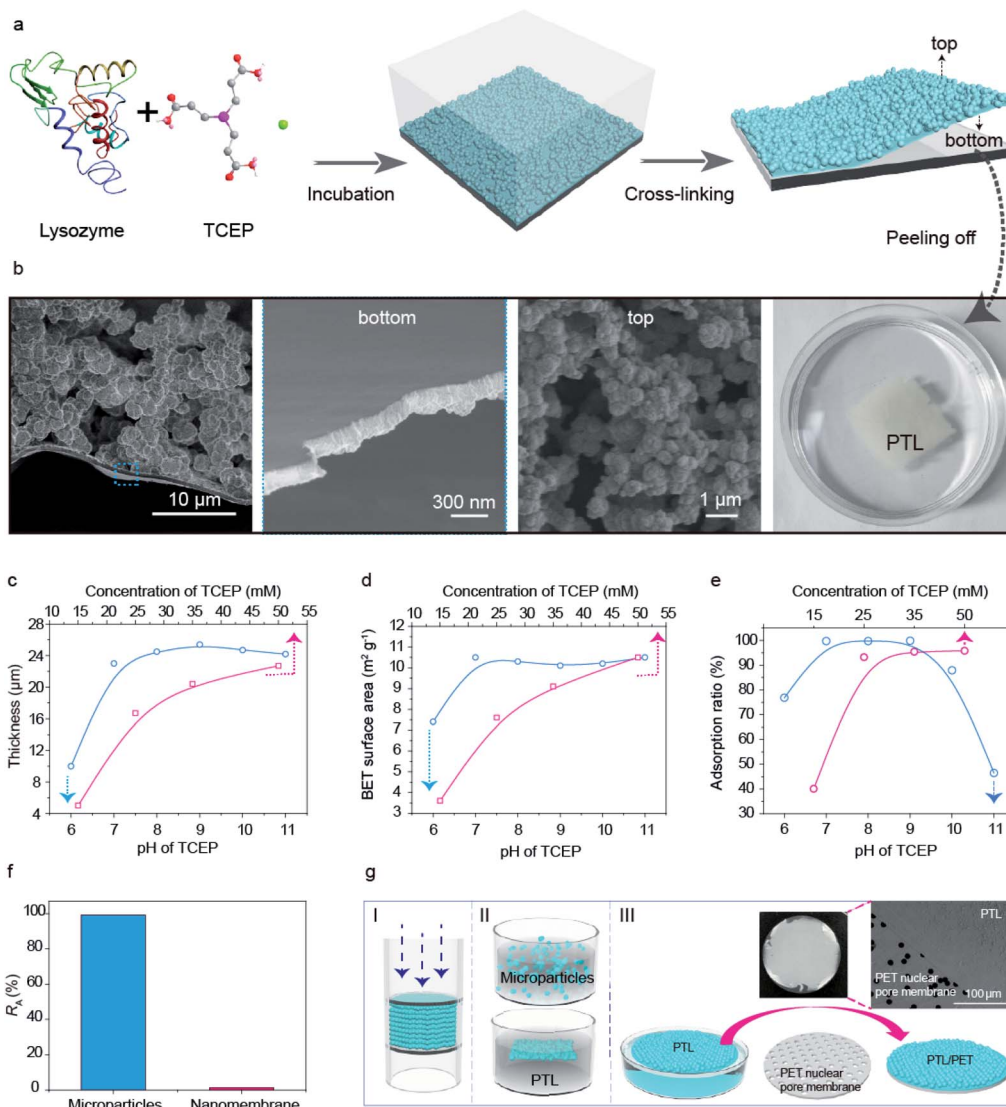
Fig. 1 Preparation and structure modulation of the PTL bilayer membrane. (a) Schematic illustration of the proposed mechanism for the preparation of the amyloid-like PTL bilayer membrane; (b) SEM image showing the cross-section of the proteinaceous bilayer membrane, consisting of two parts: a bottom SEM image showing the cross-section of the nanomembrane and a top SEM image showing the microparticles on the membrane as well as an optical photograph of the membrane (far right); (c) the effect of the concentration and pH of TCEP buffer on membrane thickness; (d) the effect of the concentration and pH of TCEP buffer on the BET specific surface area of the membrane; (e) the effect of the pH and concentration of TCEP buffer on the adsorption ratio for gold ions; (f) the adsorption ratio of gold ions on microparticles alone and the nanomembrane alone; (g) a cartoon indicating the use of microparticles as fillers in the adsorption column (I), microparticles and the PTL bilayer membrane dispersed in solution as adsorbents (II), and the attachment of the bilayer membrane onto a PET nuclear pore membrane (PTL/PET) (III). The inset shows the corresponding optical and SEM images of the PTL/PET membrane.

Therefore, to achieve high adsorption of gold ions, the optimum preparation conditions for the bilayer membrane were neutral or weakly basic TCEP.

The advantages of the bilayer membrane design were further evaluated. First, the bilayer design facilitated the collection and recovery of the adsorbent after use without detectable material loss. In comparison, although direct dispersion of the microparticles (without a nanomembrane support beneath) in the extraction solution also showed a high R_A (>95%) (Fig. 1f), such dispersion easily resulted in the loss of microparticles during recovery and utilization (Fig. S6a, ESI†). Second, when the

microparticles without a nanomembrane beneath as a support were utilized as filler in a separation column, the corresponding R_A was approximately 75% (Fig. S6b, ESI†), and this decreased R_A (compared with $R_A > 95\%$ for the bilayer design) was due to the slow diffusion of gold ions through the densely packed microparticles in the column. Third, the bottom nano-membrane is helpful for attaching the bilayer membrane robustly onto the polyethylene terephthalate (PET) nuclear pore membrane (PTL/PET) due to the multiplex interfacial bonding of the PTL nanomembrane with the other material (Fig. 1g).[28] Through such fabrication, recirculating adsorption by the PTL/

3440 | J. Mater. Chem. A, 2020, 8, 3438–3449

This journal is © The Royal Society of Chemistry 2020

PET membrane was achieved, and a high adsorption ratio of 99.6% for gold ions was observed. Therefore, the above results demonstrated that the optimal membrane-particle bilayer composition allowed both high adsorption efficiency and easy operation for reuse at the same time.

The adsorption mechanism of gold ions on the PTL bilayer membrane

To further investigate the adsorption performance of the membrane, we exposed the membrane to HAuCl$_4$ solution at different pH values, concentrations and extraction time (Fig. 2a). Lysozyme has some positively charged amino acids (*e.g.*, eleven arginine residues and six lysine residues). These positively charged amino acids on the PTL membrane were responsible for the electrostatic interaction with the gold ions, which was effectively adjusted by the pH in the extraction solution. This was because the charge state of the membrane surface, the form of metal ions and their ionic charges strongly depended on the pH of the extraction solution. At low pH (pH 1–5), the zeta potential of the PTL membrane varied from 12.6 to −17.7 mV with an isoelectric point at pH 4.5 (Fig. 2b inset), and [AuCl$_4$]$^-$ and [AuCl$_3$(OH)]$^-$ complexes became the dominant gold ion species.[29] Accordingly, the adsorption ratio of gold ions

increased as the pH of HAuCl$_4$ solution (393.9 ppm) increased from 1.0 to 2.0 and slightly decreased at pH 4.0 (R_A > 90%), at which the membrane surface net charge was close to zero (Fig. 2b). At pH 5 and above, [AuCl(OH)$_3$]$^-$ and [Au(OH)$_4$]$^-$ anions were the dominant species[30] and the surface of the membrane became negatively charged due to the deprotonation process (*i.e.*, COOH ⇔ COO$^-$ + H$^+$). The resultant electrostatic repulsion between gold ions and the membrane surface then decreased the adsorption capacity for gold ions. The above results indicated that the protein membrane was stable with a high adsorption ratio for gold ions under acidic conditions. In the following experiments examining the adsorption capacity, a pH value of 3.0 was chosen to study the theoretical maximum adsorption performance because most waste solutions containing metal ions are acidic.

The adsorption kinetics depend on the mass transfer of metal ions from the bulk solution phase to the binding sites on the surface of or inside the solid adsorbents. In this process, the adsorption ratio of gold ions on the membrane increased sharply to 80% within the first 10 min, then rose slowly and reached equilibrium above 90% after 30 min at an initial HAuCl$_4$ concentration < 50 ppm. When the initial HAuCl$_4$ concentration increased from 50 to 295.5 ppm, the adsorption time was extended to 5 h to reach equilibrium. With an increase
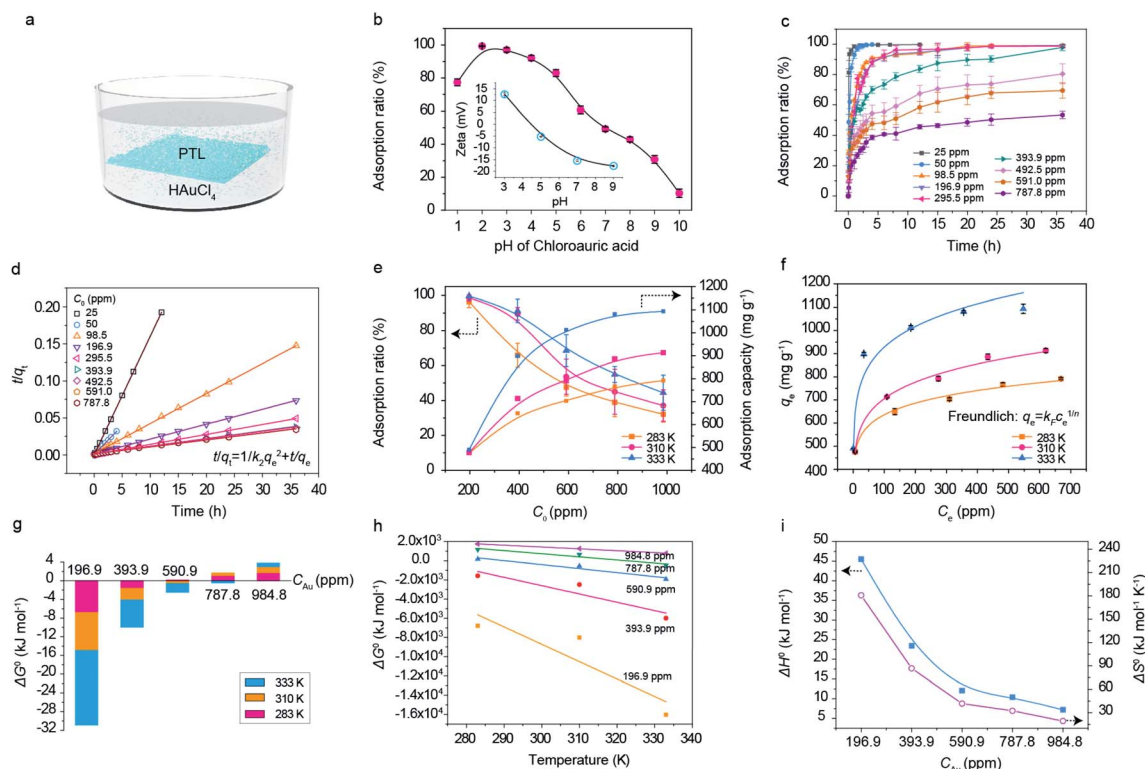

Fig. 2 The adsorption behavior of gold ions on the protein membrane. (a) Schematic illustration of the PTL adsorbent soaked in solution; (b) the gold adsorption ratio on the membrane as a function of the initial pH of HAuCl$_4$ solution. The inset shows the zeta potential of the PTL membrane in HAuCl$_4$ solution at different pH values; (c) time-dependent gold adsorption ratio at different initial [AuCl$_4$]$^-$ concentrations; (d) the adsorption kinetics fitting; (e) the gold adsorption ratio and corresponding adsorption capacity per unit mass of adsorbent (mg g^{-1}) on the membrane as a function of concentration of [AuCl$_4$]$^-$ at different temperatures; (f) the Freundlich adsorption isotherm model fitting for [AuCl$_4$]$^-$ adsorption on the membrane at three different temperatures; (g–i) thermodynamic parameters of gold ion adsorption on the membrane, including the change in Gibbs free energy (ΔG^0), enthalpy (ΔH^0) and entropy (ΔS^0). The data are presented as the means ± s.d. ($n = 3$).

in the initial gold ion concentration above 295.5 ppm, the adsorption time was extended to 24 h to reach equilibrium (Fig. 2c). The time-dependent adsorption data at different gold ion concentrations were fitted well by a pseudo-second-order kinetics model (correlation coefficient $R_2^2 > R_1^2$) (Fig. 2d, S7 and Table S1, ESI†), which showed that chemisorption was the principal uptake mechanism during this adsorption process.[29,31] The adsorption model was then evaluated by studying the effect of the temperature and the initial $HAuCl_4$ concentration on the adsorption behaviors. The adsorption capacity increased with increasing temperature, showing a considerable adsorption capacity for gold ions in the range from 758.1 mg g^{-1} to 1034.4 mg g^{-1} with increasing operation temperature from 283 K to 333 K (Fig. 2e). It is worth highlighting that, by extrapolation from the experimental values, a ~66 L volume of water with gold ions could be processed using just 2.1 mg PTL at a concentration of gold ions of 30 ppm. That is, 1 g PTL membrane could be used to treat 30 000 L of aqueous solution of gold ions. The Freundlich model fitted the isothermal adsorption data better than the Langmuir model (correlation coefficient $R_F^2 > R_L^2$), indicating that elevated temperature could enhance adsorption due to the increase in surface activity and kinetic energy of the solute (Fig. 2f, S8 and Table S2, ESI†).[32] In addition, compared with the adsorption equilibrium time of gold ions on the membrane at 310 K (24 h), the adsorption time was decreased to 15 h when the initial gold ion concentration was 787.8 ppm with pH 2.5 at 333 K (Fig. S9, ESI†). Therefore, increasing the temperature is also beneficial to reduce the adsorption time of gold ions.

The Van't Hoff equation was further employed ($\Delta G^0 = -RT \ln K_C$, K_C is the distribution coefficient), which derives the degree of surface coverage characteristics of an adsorbate onto an adsorbent and expresses the feasibility and spontaneous nature of the adsorption process (Table S3, ESI†).[29] At a low initial gold ion concentration (e.g., 196.9 ppm), ΔG^0 was negative at all tested temperatures (283, 310 and 333 K), which indicated spontaneous adsorption on the membrane surface (Fig. 2g). With an increase in initial gold ion concentration, the more gold ions were adsorbed on the membrane, the fewer the adsorption sites, which correspondingly increased ΔG^0 gradually. A threshold for ΔG^0 was observed at 590.9 ppm, in which ΔG^0 at 283 K was positive and ΔG^0 at 310 and 333 K remained weakly negative. A further increase in gold ion concentration to 948.8 ppm resulted in all positive ΔG^0 values at 283, 310 and 333 K. This tendency well explained the efficient adsorption of gold ions at low concentrations and favourable adsorption at high gold ion concentrations with increasing temperature (Fig. 2e and f). ΔH^0 and ΔS^0 were further derived from the intercept and slope of the plot of ΔG^0 versus T ($\Delta G^0 = \Delta H^0 - T\Delta S^0$) (Fig. 2h). Both ΔH^0 and ΔS^0 were positive and decreased with increasing gold ion concentration (Fig. 2i). The positive ΔH^0 indicated an endothermic adsorption process, which was consistent with the experimental results (Fig. 2e and f). With increased gold ion concentration, the more gold ions were adsorbed on the membrane surface, the more crowded the surface became, corresponding to the gradually decreasing heat effect. The positive ΔS^0 reflected the increased randomness at the solid–

solution interface during adsorption. This indicated that the adsorption of gold ions on the membrane was entropically driven. During the adsorption process, gold ions exchanged with water molecules on the membrane surface, and the entropy of the whole adsorption process became positive due to the desorption of water molecules.[29] In addition, the mobility of gold ions on the membrane surface was gradually limited as the concentration of gold ions increased; thus, ΔS^0 decreased gradually.

During the adsorption of gold ions, the color of the membrane changed rapidly from white to brown within 1 h at 310 K, in contrast to the yellow color of the membrane after adsorption at 283 K. This result indicated a possible reduction reaction for gold ions accompanying the adsorption process. The standard reduction potential of Au^{3+}/Au^+ (1.4 V) is higher than that of Au^{3+}/Au^0 (1.0 V). Hence, Au^{3+} was first reduced to Au^+, and Au^+ was then gradually reduced to Au^0. The corresponding XPS evidence showed a clear $Au^{3+} \rightarrow Au^+ \rightarrow Au^0$ stepwise reduction at different adsorption and reduction stages (Fig. S10, ESI†). A fast reduction rate was observed at 333 K, in which 89.7% Au^{3+} was reduced to Au^+ in 10 min (Fig. 3a). After 60 min, a purple product was formed on the membrane surface containing 42.3% Au^0, and no Au^{3+} species was detected, a sign of the complete reduction of Au^{3+} to Au^0 and Au^+. Furthermore, after 12 h, the Au^+ species decreased to 10%, while the Au^0 species increased to 90% (Fig. 3a and S10b, ESI†). Elevated temperature also favored such reduction, as the magnitude of the Au^0 peak increased from 19.7:87.4:3.9 ($Au^{3+}:Au^+:Au^0$) at 283 K to 0:28.3:71.7 ($Au^{3+}:Au^+:Au^0$) at 333 K (Fig. S11, ESI†). TEM images of the membrane after adsorbing and reducing gold ions then showed the existence of gold nanoparticles on the membrane surface, which gradually became larger, and the number of large particles increased with increasing temperature (Fig. S12, ESI†). The typical sizes of gold particles formed on the membrane ranged from the nanometer to micrometer scale (Fig. 3b). The spontaneous reduction ability of the protein membrane for gold ions at low temperature (~333 K) completely avoided the use of any other reductants, which in turn reduced the environmental pollution caused by the use of reducing agents and energy consumption.

The chemisorption-based kinetics and Freundlich model behavior observed during adsorption and reduction implied possible physicochemical interactions between gold ions and the functional groups present on the membrane surface, such as electrostatic interactions and gold ion chelation. The XPS spectra of N_{1s} on the membrane surface before the adsorption of gold ions showed peaks at 399.6 and 400.4 eV, assigned to unprotonated amine/amide species and protonated amine species, respectively.[13] After the adsorption of gold ions, the protonated N_{1s} spectra decreased significantly from 30 min to 60 min and 6 h, which suggested the combination of protonated amino groups (e.g., arginine residues) and gold ions due to electrostatic interactions (Fig. 3c). Lysozyme contains tryptophan (Trp) (6), histidine (His) (1), aspartic acid (Asp) (7) and tyrosine (Tyr) (3) residues (Fig. 3d), which are important for reducing gold ions and affect the reduction rate.[33–36] To further investigate the amino acid residues responsible for the fast

3442 | J. Mater. Chem. A, 2020, 8, 3438–3449

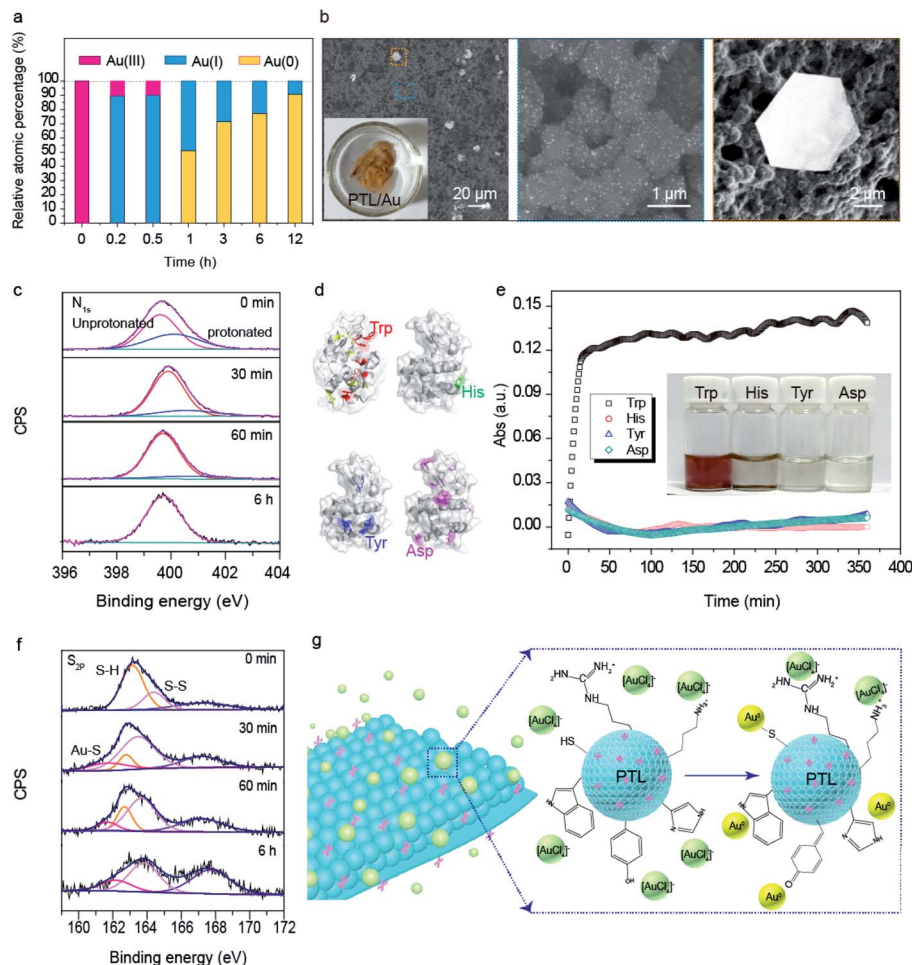This journal is © The Royal Society of Chemistry 2020

Paper

Fig. 3 The reduction of gold ions by the PTL membrane. (a) Relative atomic percentage representing the atomic fraction per total Au content for Au^{3+}, Au^+ and Au^0 at different time from the XPS spectra of Au_{4f} at 333 K; (b) SEM images showing the membrane after adsorbing and reducing gold ions. An optical photograph of the membrane after adsorbing gold ions (inset) and the typical shape and size of Au nanoparticles on the membrane are shown; (c) XPS spectra of N_{1s} after gold adsorption at 0 min, 30 min, 60 min and 6 h; (d) 3D molecular model showing tryptophan (Trp), tyrosine (Tyr), histidine (His), and aspartic acid (Asp); (e) the reduction of $[AuCl_4]^-$ by 0.1 mM Trp, Tyr, His or Asp at different time, as reflected by the UV/vis absorption of $HAuCl_4$ solution (1 mM) at 510 nm. The inset photograph shows a mixture of $HAuCl_4$ (1 mM) and amino acid (0.1 mM) solution after reduction for 6 h; (f) XPS spectra of S_{2p} on the membrane surface after gold adsorption at 0 min, 30 min, 60 min and 6 h; (g) scheme of the process by which the membrane mediates gold ion adsorption and reduction.

reducing effect in our system, the amino acids (Trp, His, Tyr and Asp) were tested individually because the functional groups (*e.g.*, imidazole, indolyl, carboxyl) of these amino acids have the potential to reduce gold ions.[19,37,38] Among these amino acids, the reduction rate of Trp for gold ions, as reflected by the UV/vis adsorption of $HAuCl_4$ solution with Trp added at 510 nm, was the fastest, with gold nanoparticles being produced within 5 minutes (Fig. 3e and S13, ESI†). For histidine and tyrosine to reduce gold, a long time was required, and the solution color changed only after 6 h due to the formation of small number of gold nanoparticles in the solutions (Fig. 3e, inset). In combination with the characteristic exposure of Trp during the phase transition of lysozyme,[21,22] it was deduced that the rapid reduction of gold ions on the bilayer PTL membrane may be mainly caused by the interaction of gold ions with the exposed Trp after the disruption of the disulfide bonds of lysozyme by TCEP.[39] In addition to Trp, the reduction of gold ions by the

membrane might be accompanied by effects exerted by His, Tyr and Asp residues, although the reduction rates of these amino acids for gold ions were much slower than that of Trp (Fig. 3e and S13, ESI†). Once the reduction product (Au^0) and resultant nanoparticles formed on the membrane surface, they were quickly stabilized by the formation of Au–S bonds between Au^0 and the 8 cysteine (Cys) residues in lysozyme; Cys residue is an important group for stabilizing Au nanoparticles due to the strong coordination between Au and thiol groups.[40] This assessment was confirmed by the high-resolution S_{2p} XPS spectra of the membrane (Fig. 3f), in which the peak at 162.1 eV, representing the presence of Au–S, appeared and was enhanced on the membrane after gold adsorption and reduction. Overall, a possible adsorption mechanism of gold ions on the membrane could be proposed based on the above results: $[AuCl_4]^-$ in acidic media was electrostatically adsorbed on the protonated groups of the membrane or positively charged

This journal is © The Royal Society of Chemistry 2020

J. Mater. Chem. A, 2020, **8**, 3438–3449 | **3443**

surfaces of the membrane. Then, Au^{3+} was reduced to metallic gold by amino acids (*e.g.*, Trp, His, Tyr and Asp), and the resultant Au nanoparticles were stabilized on the PTL by the formation of Au–S bonds *via* cysteine residues (Fig. 3g and S14, ESI†).

Competitive adsorption of precious metals in the presence of common metal ions and anions

Gold ion (Au^{3+}) adsorption was then evaluated in the presence of other competitive metal ions, including some common cations in water (Mg^{2+}, Cu^{2+}, Ni^{2+} and Zn^{2+}) and cations in minerals (Sn^{2+}, Fe^{3+}, Co^{2+}, Al^{3+}, Cr^{3+}, Bi^{2+}, Sb^{2+} and Li^+). With the existence of competitive metal ions at 100 ppm each, the adsorption ratio for gold ions at concentrations from 0.1 to 100 ppm was consistently as high as >90% (Fig. 4a). Such capability for the selective adsorption of Au^{3+} from a mixture of metal ions at a 1–1000-fold higher concentration would be practically useful for the separation of Au^{3+} from mixture solutions at a low gold ion concentration. This high selectivity was attributed to the distinctive ionic form of gold ions from

that of other competitive metal ions: at an acidic $HAuCl_4$ solution pH, the gold ions existed as $[AuCl_4]^-$ and $[AuCl_3(OH)]^-$ complexes, favoring electrostatic interactions with the positively charged membrane surface; in contrast, the other competitive common metal ions existed in the solution as cations, which would not support effective electrostatic attraction with the positively charged membrane surface.[41] In addition to widely existing cations, the most common anions widely found in tap and civil water, such as Cl^-, NO_3^- and SO_4^{2-}, would also not affect the adsorption ratio for gold ions because Au^{3+} is a soft metal ion that has a higher affinity for donor atoms such as O, N and S on the membrane surface. A high adsorption ratio > 90% was observed in the presence of these anions, indicating potential compatibility with tap and civil water (Fig. 4b).

In addition to gold ions, the membrane further showed the general ability to extract other primary precious metal ions. Since most waste solutions containing metal ions are acidic (pH < 3), the adsorption of metal ions on the membrane was studied by diluting a platinum group metal standard solution (1000 ppm Pd, Ir, Os, Pt, Ru or Rh in 2 M HCl, 1000 ppm Ag in 1% HNO_3) in
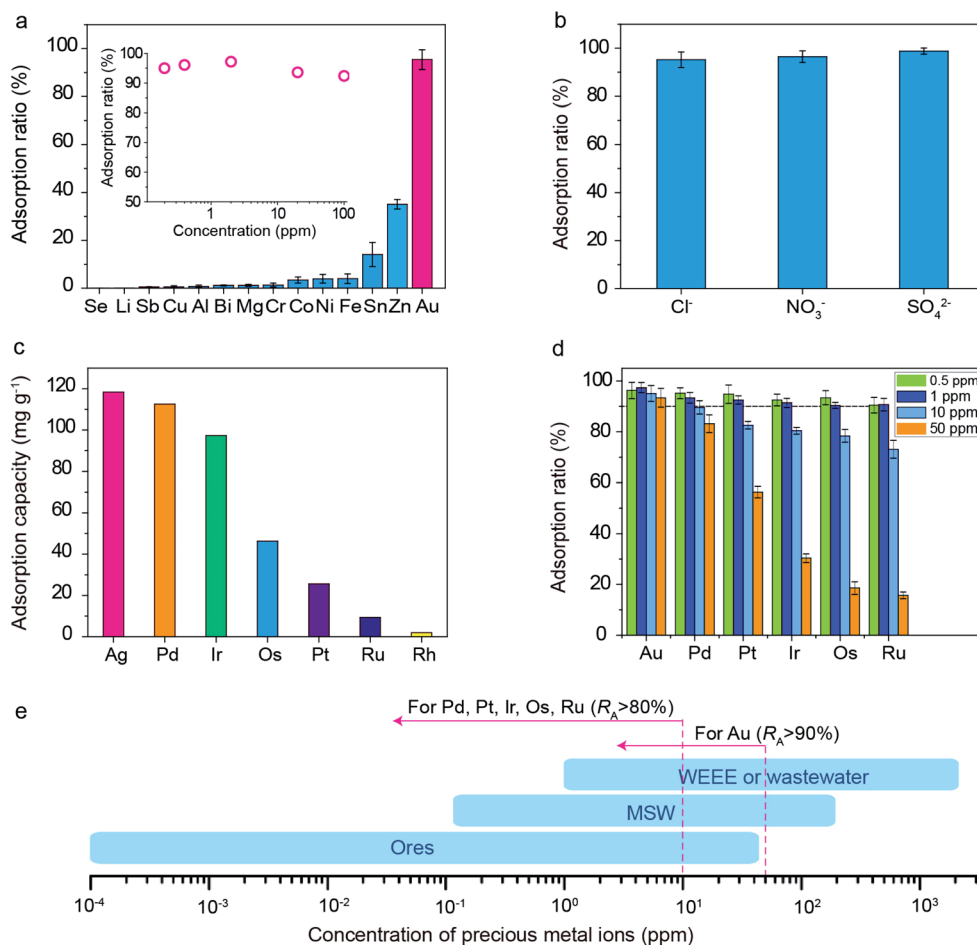

Fig. 4 The adsorption of precious metal ions by the PTL bilayer membrane. (a) The effect of competing metal ions (100 ppm each) on gold ion adsorption; the inset shows the adsorption of gold ions with different concentrations in a mixed metal ion solution; (b) the effect of Cl^-, NO_3^- and SO_4^{2-} (0.01 M) on gold adsorption; (c) adsorption capacity of the membrane for precious metals in a single system; (d) effect of initial precious metal ion concentration on adsorption in a mixed system; (e) the content of primary precious metals in ores, municipal solid waste (MSW), waste electrical and electronic equipment (WEEE) and industrial wastewater.

1% HNO_3 solution. For the adsorption trials of single precious metal ions, the adsorption capacities were 118.3, 112.5, 97.3, 46.3, 25.6, 9.4 and 2.0 mg g^{-1} for Ag, Pd, Ir, Os, Pt, Ru and Rh on the membrane, respectively. The membrane had a high adsorption capacity for Ag since Ag^+ shows an affinity for soft bases with donor atoms (O, N, or S) in amino acids such as His, Trp and Cys in proteins, according to hard–soft acid–base theory.[42,43] The adsorption of platinum group metals followed this order: Pd > Ir > Os > Pt > Ru > Rh (Fig. 4c and S15a, ESI†), suggesting that the membrane could effectively adsorb platinum group precious metal ions by electrostatic interactions due to the formation of metal–chloro complexes between the precious metal ions and chloride ions under acidic conditions. The reason for the adsorption sequence of Pd > Ir > Os > Pt > Ru > Rh is that precious metal–chloro complexes with low charge density are more easily paired than species with high charge density since low-charge species with smaller hydration shells have greater coulombic interactions with their counter ions than do those with larger hydration shells (Table S4, ESI†).[44] With a comparable adsorption capacity towards precious metals to those of existing adsorbents, the PTL bilayer membrane showed a remarkable efficiency to adsorb an extremely low level of precious metal ions (<1 ppm for Pd, Pt, Ir, Os and Ru; <50 ppm for Au) in the mixed precious metal ion solution (Fig. 4d). Silver can precipitate in the presence of Cl^-; hence, silver was not included in this mixed solution. When precious metal ions coexisted with other metal ions, the membrane showed good selectivity to precious metals (Fig. S15b, ESI†). The result encouraged the practical use of the membrane for the extraction of precious metals from ores, MSW, WEEE or industrial wastewater (e.g., spent electroplating solution is regarded as a great environmental problem, although this kind of wastewater contains many precious metals), among which the

average concentration of precious metals found in actual primary natural ores is approximately 1–40 ppm, while secondary sources (MSW, WEEE or industrial wastewater) have higher concentrations of approximately 1–2000 ppm (Fig. 4e).[45] The adsorbed precious metals on the membrane can be recovered through the desorption in acid thiourea, halide, thiosulfate or diluted acid.[46] For instance, the adsorbed Pd, Pt, Ru, Ir, Os and Rh on the membrane could be desorbed by 1 wt% thiourea in 1 M HCl for 12 h. The desorption ratio of Pd, Pt, Ru, Ir, Os and Rh was 88.2%, 96.4%, 73.5%, 80.3%, 78.1% and 68.9%, respectively. The precious metal ions in resultant eluent solution after the desorption can be further separated from each other by exploiting differences in the chemistry of their anionic chloro-complexes, including solvent extraction, ion exchange, precipitation and crystallization.[44] For instance, the amine-based extractants (e.g., alamine, aliquat) have been extensively employed for the extraction and recovery of Pt from the complex chloride solutions in the presence of various anionic and cationic species.[47] For Ir, Ru and Os, they can form volatile oxides under strongly oxidizing conditions which enable their separation from other precious metals by distillation; further, OsO_4 is more stable than RuO_4 and selective reduction of RuO_4 by dissolution in HCl enables separation of these two metals.[44]

To further evaluate the potential practical application of the membrane for the extraction of precious metals from ores or WEEE (e.g., mobile phones), we carried out comprehensive adsorption from leaching solution containing a variety of competing ions. First, we used gold ore as a raw material to develop a laboratory-scale gold extraction process. Using a gold leaching solution prepared through the complete extraction of gold ore by the aqua regia method (the volume ratio of concentrated HNO_3 to concentrated HCl was 1 : 3), the
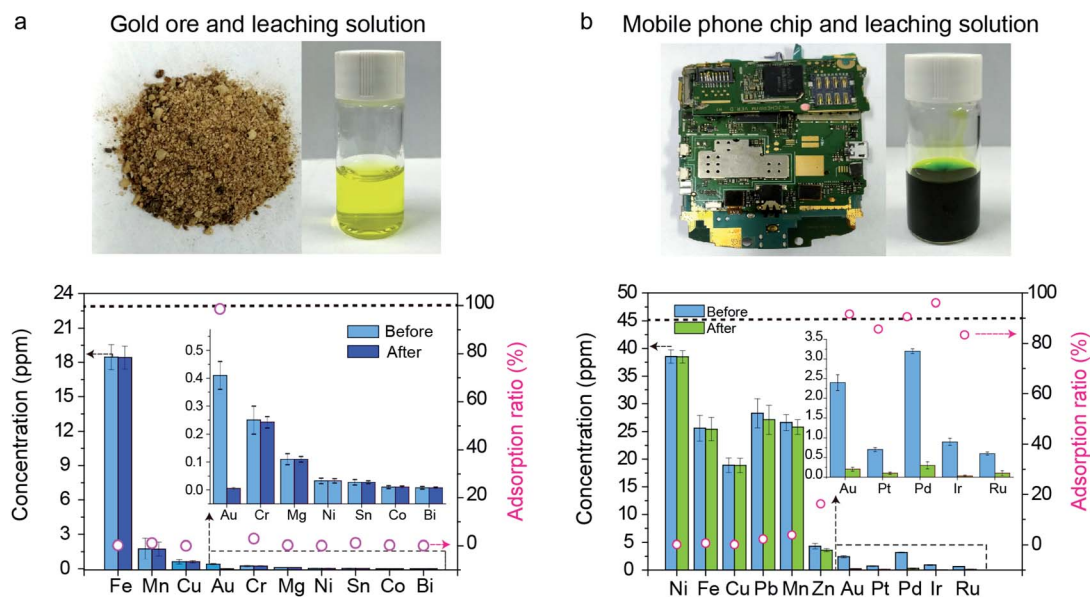

Fig. 5 The adsorption of precious metal ions by the PTL bilayer membrane. (a) Photograph of gold ore and the corresponding leaching solution (top). The effect of competing metal ions on gold adsorption in gold leaching solution from ore (bottom); (b) photograph of a mobile phone chip and the corresponding leaching solution (top). The effect of competing metal ions on the adsorption of precious metals in leaching solution from mobile phone chips (bottom).

adsorption of gold ions was tested after diluting the leachate to different degrees due to the high acidity of aqua regia. The adsorption ratio reached 73.2% for 0.4 ppm gold (40-fold dilution) at pH 1.0 after 12 h (Fig. S16a, ESI†). In contrast, when the pH of the leachate solution was adjusted to 2.0, the membrane was able to extract 75.6% of 0.4 ppm gold in less than 30 min and then reached 90% removal in 2 h (Fig. 5a and S16b, ESI†). The high adsorption ratio was selective for Au, while the adsorption of other competing metal ions contained in the leachate solution of gold ores, such as Fe, Mn, Cu, Cr, Mg, Ni, Sn, Co, and Bi, remained slight. Second, we further used the membrane to extract the precious metals from mobile phone chips. For this aim, mobile phone chips were fully leached by aqua regia, and the leachate solution was then extracted by the membrane. It was found that in the presence of various common cations (Ni, Fe, Cu, Pb, Mn, and Zn), the membrane selectively adsorbed the precious metal ions from the leachate solution, including Au, Pt, Pd, Ir and Ru, at a high adsorption ratio (84–95%) (Fig. 5b). With the dilution of the leachate

solution by 50 times (1.4 ppm Au), the adsorption ratio for gold was close to 100% after 30 min (Fig. S17, ESI†). The above results thus indicated that the membrane had a fast and highly efficient capability for the extraction of precious metal ions from diluted leachate solutions of gold ores and WEEE.

Strategies for the recovery of gold ions and regeneration of the membrane

Desorption and reuse ability is an important property for cost-effective biosorbents.[48] As mentioned above, the bottom of the nanomembrane in the bilayer of the PTL adsorbent could be adhered onto a PET nuclear pore membrane (PTL/PET) due to the multiplex interfacial bonding of the nanomembrane with this material. This composite membrane could then be directly used to conduct adsorption–desorption cycles for gold ions (Fig. 6a). We investigated the desorption of Au^0 from the PTL/PET membrane by using eluent solution containing a combination of thiourea (130 mM), ammonium thiocyanate (780 mM)
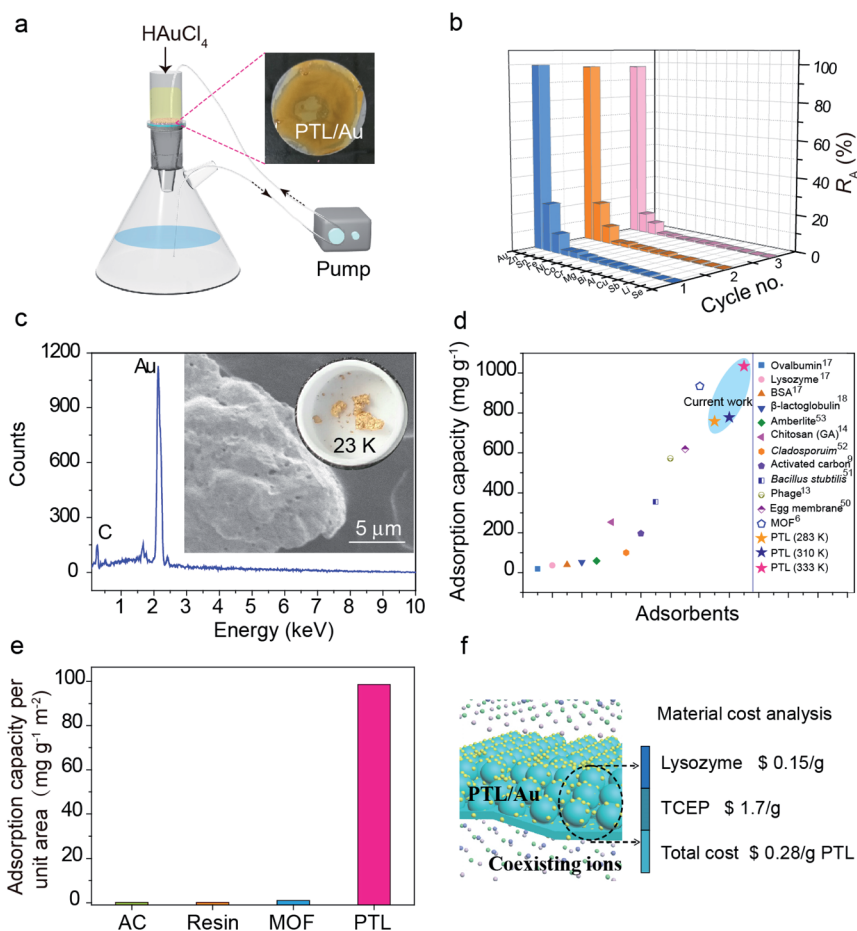

Fig. 6 Desorption and recovery of gold ions. (a) Schematic for cyclic adsorption on the PTL/PET membrane and an optical photograph of the membrane after the adsorption of gold ions (top right); (b) reuse of the desorbed PTL/PET membrane for the cyclic adsorption of gold ions; (c) SEM image and photograph of the final reduced gold powder (23 K) after pyrolysis of the sample at 900 °C for 5 h and the corresponding EDX spectrum of the resultant Au agglomerate at a purity of 96%; (d) comparison of gold adsorption capacity among different adsorbents. The experimental value in the current work is compared with literature values for other adsorbents; (e) the adsorption capacity per unit area for gold by using activated carbon (AC),[9] an ion exchange resin (Amberlite),[53] an MOF[6] and the PTL bilayer membrane; (f) scheme and material cost analysis of the PTL membrane system for gold adsorption.

3446 | J. Mater. Chem. A, 2020, 8, 3438–3449

This journal is © The Royal Society of Chemistry 2020

and ferric sulfate (28 mM).[48] In this system, the adsorbed Au^0 can be oxidized to Au^+ by using Fe^{3+} as the oxidant, and then Au^+ will complex with thiourea/SCN^- to form stable complexation ions that are dissolved in the solution.[5] After desorption, the color of the composite membrane changed from golden brown to white, and the gold sheets on the surface of the membrane were completely desorbed without affecting the surface morphology of the membrane (Fig. S18a–c, ESI†). The resultant Au–SCN complex could be further reduced by sodium borohydride to collect Au(0) metal. For this aim, the solution containing Au(III) complex was added by sodium borohydride (2 mg mL^{-1}) and continuously agitating for 30 min at room temperature. The resultant recovery ratio for the adsorbed gold from the membrane was over 90% with the existence of other metal ions at 50 ppm each, and the adsorption ratio of the regenerated membrane in the next extraction of gold ions was still above 90% after three rounds of desorption (Fig. 6b). The thiourea desorption has been widely utilized in hydrometallurgy industry,[49] and could be further simplified by an alternative method reported by our group in 2017.[4] In such a simplified method, an aqueous solution of *N*-bromosuccinimide (NBS) and pyridine (Py) at near-neutral pH was utilized to directly leach Au(0) from gold ore and electronic waste to form Au(III) in water.[4] This oxidative leaching process was more environmentally benign and simpler than the classical thiourea method, achieving the desorption performance nearly as same as that from the thiourea method. To directly recover gold ions into metallic form with high purity, a combined adsorption-incineration process can be further applied, in which ionic Au can be reduced to metallic form along with the oxidation of organic constituents during incineration. Because gold is more expensive than other common metals and lysozyme is less inexpensive than synthetic resins, the sorption-incineration method can be a good and economic option for the recovery of gold from PTL. After the gold-loaded PTL was incinerated to remove organic constituents and directly recover zero-valent gold from the Au-loaded PTL, we achieved a gold recovery of 96%. Upon further pyrolysis to decompose carbonaceous impurities, the purity of the final obtained gold was 23 K (95.8 wt%), which represents a precious gold value (Fig. 6c).

The PTL bilayer membrane showed the highest adsorption capacity among other alternatives, such as native proteins,[17,18] eggshell membranes,[50] bacteria (*e.g.*, *Bacillus subtilis*),[51] fungi (*e.g.*, *Cladosporium cladosporoides*),[52] phages,[13] and MOFs (metal–organic frameworks),[6] and the adsorption capacity was significantly higher than that of traditional most-utilized industrial synthetic materials, such as activated carbon (AC) and ion exchange resins (*e.g.*, Amberlite)[53] (Fig. 6d). Although activated carbon, ion exchange resins and MOFs may have a larger BET surface area than the PTL bilayer membrane, the adsorption capacity per unit area of the bilayer membrane was 100–500 times greater than that of activated carbon, ion exchange resins and MOFs (Fig. 6e and S19, ESI†).

Based on the laboratory price for the reagents required to prepare the PTL membrane, easy preparation procedure and high reusability of the membrane, the cost of gold adsorption based on our system was estimated to be comparable with that of activated carbon. For instance, by extrapolating the experimental capacity of the PTL membrane, the PTL had a cumulative adsorption capacity of up to 3.1 kg gold after recycling by using 1 g of PTL ($ 0.28$), while 18 g of activated carbon ($ 0.26$) would have to be used to adsorb the same amount of gold (Fig. 6f). In addition to the advantageous adsorption capacity and price, the fast kinetics, high selectivity and mild preparation/regeneration conditions, as well as spontaneous reduction capability without the need for additional reductants, substantially reduced the energy consumption for the PTL-based adsorbent.

Conclusions

In summary, the well-defined bilayer PTL membrane comprising top microparticle and bottom nanomembrane layers, could be used to recover precious metals, especially gold ions, at a high efficiency and without the use of any other synthetic reductants. The adsorption mechanism is generally regarded to comprise physicochemical interactions between metal ions and the functional groups present on the surface of the proteinaceous membrane, typically including electrostatic interactions, metal ion chelation or complexation and *in situ* reduction on the membrane surface. The membrane showed a high adsorption capacity of 1034.4 mg g^{-1} for gold ions and can be used for multiple cycles of sorption–desorption. The adsorption capacity of the PTL membrane for gold was 3–15 times higher than that of activated carbon (the most-utilized adsorbent), ion exchange resins and MOFs. In addition to gold ions, the PTL membrane could be easily utilized as a commercially viable method to simultaneously extract a variety of primary precious metals from diluted precious metal-containing solution (*e.g.*, with concentrations of 0.5 to 10 ppm) in the presence of a large amount of competing metal ions. This research highlights the potential application of a green technology for the economic extraction of trace precious metals from ores, industrial and civil waste solid and liquid by using the proposed pure amyloid-like protein bilayer membrane, which can efficiently reduce secondary pollution and meet the targets of a circular economy and bioresource reutilization.

In the future, it is promising to further functionalize the membrane to improve the selectivity towards individual precious metals. The multiple functional groups on the membrane surface including hydroxyl, carboxyl, thiol and amine groups can be substituted with desirable functional structures by various chemical surface modifications to improve the adsorption selectivity of individual precious metals. For example, α-cyclodextrin showed high selectivity to gold ions in the presence of other precious metals,[15] hence, it can be achieved by grafting α-cyclodextrin on the protein membrane to selectively adsorb gold ions. It was also reported that Pd(II) could complex with benzimidazole, crown ethers or sulfur-containing ligands,[54] so it is feasible to introduce these structures on the membrane surface to selectively bind with Pd(II). In addition to, elimination of interfering sites from the membrane could produce better selectivity, such as methylation of amine

This journal is © The Royal Society of Chemistry 2020

J. Mater. Chem. A, 2020, **8**, 3438–3449 | **3447**

groups, acetylation of amine and hydroxyl groups and esterification of carboxyl groups.[45]

Conflicts of interest

The Shaanxi Normal University has applied for a patent for the discussed membrane materials and related applications with P. Y. and F. Y. listed as the inventors. The remaining authors declare no competing interests.

Acknowledgements

Notes and references

1 G. Hutchings, *Nat. Chem.*, 2009, **1**, 584.

2 M. Mon, J. Ferrando-Soria, T. Grancha, F. R. Fortea-Pérez, J. Gascon, A. Leyva-Pérez, D. Armentano and E. Pardo, *J. Am. Chem. Soc.*, 2016, **138**, 7864–7867.

3 J. E. Zweig, D. E. Kim and T. R. Newhouse, *Chem. Rev.*, 2017, **117**, 11680–11752.

4 C. Yue, H. Sun, W. J. Liu, B. Guan, X. Deng, X. Zhang and P. Yang, *Angew. Chem., Int. Ed.*, 2017, **56**, 9331–9335.

5 (*a*) A. M. Wilson, P. J. Bailey, P. A. Tasker, J. R. Turkington, R. A. Grant and J. B. Love, *Chem. Soc. Rev.*, 2014, **43**, 123–134; (*b*) E. D. Doidge, I. Carson, P. A. Tasker, R. J. Ellis, C. A. Morrison and J. B. Love, *Angew. Chem., Int. Ed.*, 2016, **55**, 12436–12439.

6 D. T. Sun, N. Gasilova, S. Yang, E. Oveisi and W. Queen, *J. Am. Chem. Soc.*, 2018, **140**, 16697–16703.

7 X. Chen, K. F. Lam, S. F. Mak and K. L. Yeung, *J. Hazard. Mater.*, 2011, **186**, 1902–1910.

8 C. Mack, B. Wilhelmi, J. R. Duncan and J. E. Burgess, *Biotechnol. Adv.*, 2007, **25**, 264–271.

9 C. A. Snyders, S. M. Bradshaw, G. Akdogan and J. J. Eksteen, *Hydrometallurgy*, 2014, **149**, 132–142.

10 H. A. Alhashimi and C. B. Aktas, *Resour., Conserv. Recycl.*, 2017, **118**, 13–26.

11 S. Meyer, B. Glaser and P. Quicker, *Environ. Sci. Technol.*, 2011, **45**, 9473–9483.

12 M. M. Titirici, R. J. White, C. Falco and M. Sevilla, *Energy Environ. Sci.*, 2012, **5**, 6796–6822.

13 M. I. Setyawati, J. Xie and D. T. Leong, *ACS Appl. Mater. Interfaces*, 2014, **6**, 910–917.

14 S. I. Park, I. S. Kwak, S. W. Won and Y. S. Yun, *J. Hazard. Mater.*, 2013, **248**, 211–218.

15 Z. Liu, M. Frasconi, J. Lei, Z. J. Brown, Z. Zhu, D. Cao, J. Iehl, G. Liu, A. C. Fahrenbach, Y. Y. Botros, O. K. Farha, J. T. Hupp, C. A. Mirkin and J. F. Stoddart, *Nat. Commun.*, 2013, **4**, 1855.

16 J. R. Dodson, H. L. Parker, A. M. García, A. Hicken, K. Asemave, T. J. Farmer, H. He, J. H. Clark and A. J. Hunt, *Green Chem.*, 2015, **17**, 1951–1965.

17 T. Maruyama, H. Matsushita, Y. Shimada, I. Kamata, S. Sonokawa, N. Kamiya, N. Kamiya and M. Goto, *Environ. Sci. Technol.*, 2007, **41**, 1359–1364.

18 S. Bolisetty and R. Mezzenga, *Nat. Nanotechnol.*, 2016, **11**, 365–371.

19 J. Xie, Y. Zheng and J. Y. Ying, *J. Am. Chem. Soc.*, 2009, **131**, 888–889.

20 G. Nyström, M. P. Fernández-Ronco, S. Bolisetty, M. Mazzotti and R. Mezzenga, *Adv. Mater.*, 2016, **28**, 472–478.

21 D. Wang, Y. Ha, J. Gu, Q. Li, L. Zhang and P. Yang, *Adv. Mater.*, 2016, **28**, 7414–7423.

22 C. Li, L. Xu, Y. Zuo and P. Yang, *Biomater. Sci.*, 2018, **6**, 836–841.

23 A. Gao, Q. Wu, D. Wang, Y. Ha, Z. Chen and P. Yang, *Adv. Mater.*, 2016, **28**, 579–587.

24 Y. H. Wang, T. H. Young and T. J. Wang, *Exp. Eye Res.*, 2019, **185**, 107679.

25 J. Gu, Y. Su, P. Liu, P. Li and P. Yang, *ACS Appl. Mater. Interfaces*, 2017, **9**, 198–210.

26 Y. Shen, L. Posavec, S. Bolisetty, F. M. Hilty and R. Mezzenga, *Nat. Nanotechnol.*, 2017, **12**, 642–647.

27 S. Bolisetty, J. J. Vallooran, J. Adamcik, S. Handschin, F. Gramm and R. Mezzenga, *J. Colloid Interface Sci.*, 2011, **361**, 90–96.

28 F. Yang, F. Tao, C. Li, L. Gao and P. Yang, *Nat. Commun.*, 2018, **9**, 5443.

29 P. Wang, M. Du, H. Zhu, S. Bao, T. Yang and M. Zou, *J. Hazard. Mater.*, 2015, **286**, 533–544.

30 F. Moreau, G. C. Bond and A. O. Taylor, *J. Catal.*, 2005, **231**, 105–114.

31 J. Febrianto, A. N. Kosasih, J. Sunarso, Y. H. Ju, N. Indraswati and S. Ismadji, *J. Hazard. Mater.*, 2009, **162**, 616–645.

32 K. Y. Foo and B. H. Hameed, *Chem. Eng. J.*, 2010, **156**, 2–10.

33 S. Si and T. K. Mandal, *Chem.–Eur. J.*, 2007, **13**, 3160–3168.

34 R. Djalali, Y. F. Chen and H. Matsui, *J. Am. Chem. Soc.*, 2002, **124**, 13660–13661.

35 J. W. Park and J. S. Shumakerparry, *J. Am. Chem. Soc.*, 2014, **136**, 1907–1921.

36 H. Wei, Z. Wang, J. Zhang, S. House, Y. G. Gao, L. Yang, H. Robinson, L. H. Tan, H. Xing, C. Hou, I. M. Robertson, J. M. Zuo and Y. Lu, *Nat. Nanotechnol.*, 2011, **6**, 93–97.

37 Y. Shao, Y. Jin and S. Dong, *Chem. Commun.*, 2004, **10**, 1104–1105.

38 S. K. Bhargava, J. M. Booth, S. Agrawal, P. Coloe and G. Kar, *Langmuir*, 2005, **21**, 5949–5956.

39 Z. Huo, C. K. Tsung, W. Huang, X. Zhang and P. Yang, *Nano Lett.*, 2008, **8**, 2041–2044.

40 Y. Xu, J. Sherwood, Y. Qin, D. Crowley, M. Bonizzoni and Y. Bao, *Nanoscale*, 2014, **6**, 1515–1524.

41 M. Zhu, W. Zhang, Y. Li, L. Gai, J. Zhou and W. Ma, *J. Mater. Chem. A*, 2016, **4**, 19060–19069.

42 R. G. Pearson, *J. Am. Chem. Soc.*, 1963, **85**, 3533–3539.

3448 | *J. Mater. Chem. A*, 2020, **8**, 3438–3449

This journal is © The Royal Society of Chemistry 2020

43 T. Shoeib, K. W. M. Siu and A. C. Hopkinson, *J. Phys. Chem. A*, 2002, **106**, 6121–6128.

44 F. L. Bernardis, R. A. Grant and D. C. Sherrington, *React. Funct. Polym.*, 2005, **65**, 205–217.

45 S. W. Won, P. Kotte, W. Wei, A. Lim and Y. S. Yun, *Bioresour. Technol.*, 2014, **160**, 203–212.

46 M. Wang, Q. Tan, J. F. Chiang and J. Li, *Front. Environ. Sci. Eng.*, 2017, **11**, 1.

47 M. K. Jha, D. Gupta, J. C. Lee, V. Kumar and J. Jeong, *Hydrometallurgy*, 2014, **142**, 60–69.

48 A. Ramesh, H. Hasegawa, W. Sugimoto, T. Maki and K. Ueda, *Bioresour. Technol.*, 2008, **99**, 3801–3809.

49 A. C. Grosse, G. W. Dicinoski, M. J. Shaw and P. R. Haddad, *Hydrometallurgy*, 2003, **69**, 1–21.

50 S. I. Ishikawa, K. Suyama, K. Arihara and M. Itoh, *Bioresour. Technol.*, 2002, **81**, 201–206.

51 Y. Ji, G. Hong, J. Sun and C. Fang, *Chem.–Eur. J.*, 2011, **172**, 122–128.

52 A. V. Pethkar, S. K. Kulkarni and K. M. Paknikar, *Bioresour. Technol.*, 2001, **80**, 211–215.

53 N. V. Nguyen, J. C. Lee, S. K. Kim, M. K. Jha, K. S. Chung and J. Jeong, *Gold Bull.*, 2010, **43**, 200–208.

54 H. V. Ehrlich, T. M. Buslaeva and T. A. Maryutina, Trends in sorption recovery of platinum metals: a critical survey, *Russ. J. Inorg. Chem.*, 2017, **62**, 1797–1818.

This journal is © The Royal Society of Chemistry 2020

J. Mater. Chem. A, 2020, **8**, 3438–3449 | **3449**